First-principles study of the high-pressure phase transition in $ZnAl_2O_4$ and $ZnGa_2O_4$: From cubic spinel to orthorhombic post-spinel structures

Sinhué López* and A. H. Romero†
CINVESTAV-Queretaro, Libramiento Norponiente No 2000, Real de Juriquilla, 76230 Queretaro, México

P. Rodríguez-Hernández‡ and A. Muñoz§
Departamento de Física Fundamental II, MALTA Consolider Team, Instituto de Materiales y Nanotecnología, Universidad de La Laguna, La Laguna, 38205 Tenerife, Spain

(Received 14 January 2009; revised manuscript received 26 March 2009; published 3 June 2009)

In this work we present a first-principles density functional study of the electronic, vibrational, and structural properties of $ZnGa_2O_4$ and $ZnAl_2O_4$ spinel structures. Here we focus our study in the evolution of the structural properties under hydrostatic pressure. Our results show that $ZnGa_2O_4$ under pressure has a first-order phase transition to the marokite ($CaMn_2O_4$) structure, which is in good agreement with recent angle-dispersive x-ray diffraction experiments. We also report a similar study for the $ZnAl_2O_4$ spinel; we found that this compound under pressure has a first-order phase transition to the orthorhombic $CaFe_2O_4$-type structure. Our results in both compounds support, under nonhydrostatic condition, the possibility of a second-order phase transition from the cubic spinel to the tetragonal spinel as reported experimentally in $ZnGa_2O_4$.

DOI: 10.1103/PhysRevB.79.214103 PACS number(s): 61.50.Ks, 61.50.Ah, 62.50.−p, 63.20.dk

I. INTRODUCTION

Oxide spinel compounds AB_2O_4 are ceramics that have many interesting electric, mechanic, magnetic, and optical properties. These compounds have been characterized by means of theory and experiments to get a better understanding of its properties. Among all those interesting properties, the structural dependence under pressure has called a lot of attention, mainly due to their occurrence in many geological settings of the Earth's crust and mantle. Many AB_2O_4 spinels crystallize in the cubic spinel structure ($Fd\bar{3}m$) exemplified by $MgAl_2O_4$. Reid and Ringwood[1] suggested that a possible postspinel phase in $MgAl_2O_4$ would be similar to $CaFe_2O_4$-type, $CaTi_2O_4$-type, or $CaMn_2O_4$-type structures, with the space groups (SGs) *Pnma*, *Cmcm*, and *Pbcm*, respectively. Very recently Ono *et al.*[2] showed, by first-principles calculations, that cubic spinel $MgAl_2O_4$ undergoes a phase transition to orthorhombic $CaFe_2O_4$- and $CaTi_2O_4$-type structures when compressed at high pressure. However, the structure and properties of post-spinel phases are presently still under debate.

Unlike MgB_2O_4 compounds, there are only few experimental high-pressure studies about the structural characterization of cubic spinels ZnB_2O_4, $ZnAl_2O_4$,[3] $ZnFe_2O_4$,[4] and $ZnGa_2O_4$.[5] All these spinels have been recently characterized by angle-dispersive x-ray powder diffraction under high pressures. In the case of $ZnFe_2O_4$ they found that there is an evident phase transition from spinel to $CaTi_2O_4$- or $CaMn_2O_4$-type structure between 26 and 36.6 GPa, where the cubic spinel phase is practically negligible.[4] Unlike $ZnFe_2O_4$, Levy *et al.*[3] found that there is no phase transition of $ZnAl_2O_4$ up to a pressure of 43 GPa. On the other hand, $ZnGa_2O_4$ was characterized very recently by Errandonea *et al.*[5] by following the structural changes up to 56 GPa and showing clear evidence of two structural phase transitions. In their work, the $ZnGa_2O_4$ has a first second-order phase transition from the cubic spinel to a tetragonal spinel with I_{41}/amd symmetry above 31 GPa. The tetragonal spinel is the structure of $ZnMn_2O_4$ and that of $MgMn_2O_4$ at ambient pressure. Finally, a second structural phase transition was reported in $ZnGa_2O_4$ around 55 GPa from the tetragonal spinel to the orthorhombic *Pbcm* structure. This last structure corresponds to marokite ($CaMn_2O_4$) at ambient pressure.

From the theoretical side, the cubic spinels $ZnAl_2O_4$ and $ZnGa_2O_4$, have been characterized by *ab initio* calculations. The majority of reports is concentrated on the structural, electronic, elastic,[6,7,11] and vibrational properties of the $ZnAl_2O_4$ (Ref. 9) at equilibrium volume. The behavior of the structural parameters and elastic constant under pressure has been reported in Refs. 7 and 11. But to our knowledge, there is not any theoretical report concerning the study of possible phase transition induced by pressure as the ones showed by other spinel compounds.[2,5]

In this paper, we report first-principles calculations of the structural, electronic, and vibrational properties of the cubic spinels $ZnAl_2O_4$ and $ZnGa_2O_4$ compounds at zero pressure. Besides, we report the variation in the structural parameters under pressure and compare directly with recent experimental measurements. Finally, we study the possible pressure-induced structural phase transitions for both compounds.

The paper is organized as follows: computational details are described in Sec. II. The characterization results of $ZnAl_2O_4$ and $ZnGa_2O_4$ compounds at zero pressure and under pressure are presented in Secs. III A and III B, respectively. Finally, we present the conclusions of this work in Sec. IV.

II. COMPUTATIONAL DETAILS

Total energy calculations were done within the framework of the density functional theory (DFT) and the projector-augmented wave (PAW) (Refs. 12 and 13) method using the Vienna *ab initio* simulation package (VASP).[14–17] The exchange and correlation energy was described within the local

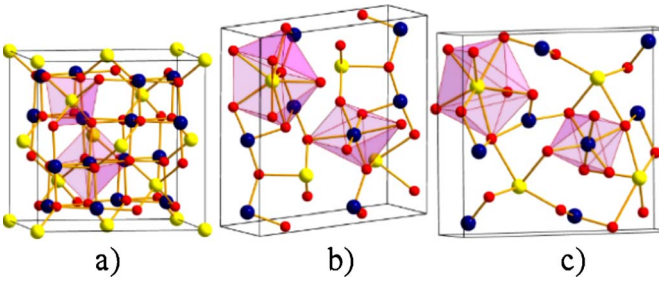

FIG. 1. (Color online) Unit cell of the AB_2O_4 structures (a) cubic spinel, (b) marokite-type, and (c) $CaFe_2O_4$-type structure. The atom color palette for A(Zn), B(Ga or Al), and O are yellow, blue, and red, respectively.

density approximation (LDA).[18] We use a 500 eV plane-wave energy cutoff to guarantee a pressure convergence to less than 2 kBar. Monkhorst-Pack scheme was employed for the Brillouin-zone integrations[19] with a mesh $4\times4\times4$, $6\times3\times3$, $8\times4\times4$, and $8\times4\times4$, which corresponds to a set of 10, 12, 16, and 16 special k points in the irreducible Brillouin-zone, for structures: cubic spinel ($Fd\bar{3}m$), tetragonal spinel (I_{41}/amd), and the orthorhombic structures with space groups *Pbcm* and *Pnma*, respectively. In the relaxed equilibrium configuration, the forces are less than 0.9 meV/Å per atom in each of the cartesian directions. The highly converged results on forces are required for the dynamical matrix calculations using the direct force-constant approach (or supercell method).[20] The construction of the dynamical matrix at the Γ point is particularly simple and involves separate force calculations, where the displacement from the atomic equilibrium configuration, within the unit cell, are considered. Symmetry aids by reducing the number of such independent distortions to six independent displacements within the cubic spinel phase. Dynamical matrices where estimated by considering positive and negative displacements ($u\approx\pm0.03$ Å). We have also checked that these displacements are within the harmonic approximation. Diagonalization of the dynamical matrix provides both the frequencies of the normal modes and their polarization vectors. It allows us to identify the irreducible representation and the character of the phonon modes at the zone center.

III. RESULTS AND DISCUSSION

A. Cubic spinels $ZnGa_2O_4$ and $ZnAl_2O_4$

Zinc gallate ($ZnGa_2O_4$) and gahnite ($ZnAl_2O_4$) crystallize at ambient pressure in a diamond-type cubic spinel structure with space-group $Fd\bar{3}m$ (227) (see Fig. 1). The A cations are tetrahedrally coordinate, and the B cations are in BO_6 octahedra. The Zn atoms are located at the Wyckoff positions, 8a (1/8,1/8,1/8) tetrahedral sites, while Ga (or Al) atoms are located on the 16d (1/2,1/2,1/2) octahedral sites and the oxygen atoms at 32e (u,u,u). The spinel crystal structure is characterized only by the lattice parameter a and the internal parameter u.

The equilibrium lattice parameters have been calculated by minimizing the crystal total energy obtained for different volumes and fitted with the Murnaghan's equation of state (EOS).[21] The calculated equilibrium lattice constants are 8.289 and 8.020 Å in good agreement with the experimental values of 8.341 Å[5] and 8.0911 Å[3] for $ZnGa_2O_4$ and $ZnAl_2O_4$, respectively. We also performed a similar study using the generalized gradient approximation (GGA) in the Perdew-Burke-Ernzerhof (PBE) (Refs. 22 and 23) exchange-correlation functional, and we have obtained similar results, with an overestimation of the lattice constant of 1.63%. Therefore, all reported results in this paper are obtained within the LDA approximation. The values of the oxygen internal-parameter u are found to be $u=0.2608$ and 0.2638, also in good agreement with the experimental values 0.2599[5] and 0.2654[3] for $ZnGa_2O_4$ and $ZnAl_2O_4$, respectively. In Table I we report our obtained structural parameters, bulk modulus B_0, bulk-modulus pressure derivative B_0', and bond distances for both compounds. Our calculated B_0 are in good agreement with experimental results and our values for B_0' are bigger than the experimental results, probably due to the experimental nonhydrostatic conditions.

TABLE I. Ground-state parameters of the spinel structures $ZnGa_2O_4$ and $ZnAl_2O_4$. Where a is the lattice parameter, u is the oxygen parameter, $d_{Zn\text{-}O}$ is the distance between Zn and O, d_{X-O} is the distance between X (Al or Ga) atom and O, B_0 is bulk modulus, and B_0' is the bulk-modulus pressure derivative.

	$ZnGa_2O_4$			$ZnAl_2O_4$		
	Present	Exp.[a]	Others	Present	Exp.[b]	Others
a (Å)	8.289	8.341	8.2506[c] 8.4063[d] 7.977[e]	8.020	8.0911	7.998[f] 8.0505[d] 8.086[g]
u	0.2608	0.2599	0.2611[c] 0.2614[d] 0.2673[e]	0.2638	0.2654	0.389[f] 0.2651[d] 0.3886[g]
$d_{Zn\text{-}O}$ (Å)	1.950	1.949	1.943[c] 1.966[e]	1.929	1.9662	1.93[f]
d_{X-O} (Å)	1.987	2.004	1.975[c] 1.866[e]	1.901	1.9064	1.89[f]
B_0 (GPa)	218.93	233	217[c] 156[d] 207.52[e]	219.65	201.7	218[f] 183[d]
B_0'	4.35	8.3	3.77[e]	4.02	7.62	

[a]Reference 5.
[b]Reference 3.
[c]Reference 6.
[d]Reference 7.
[e]Reference 8.
[f]Reference 9.
[g]Reference 10.

Figures 2(a) and 2(b) display our calculated band structure along the high-symmetry directions of the $ZnAl_2O_4$ and $ZnGa_2O_4$ compounds. These cubic spinel oxides are wide-

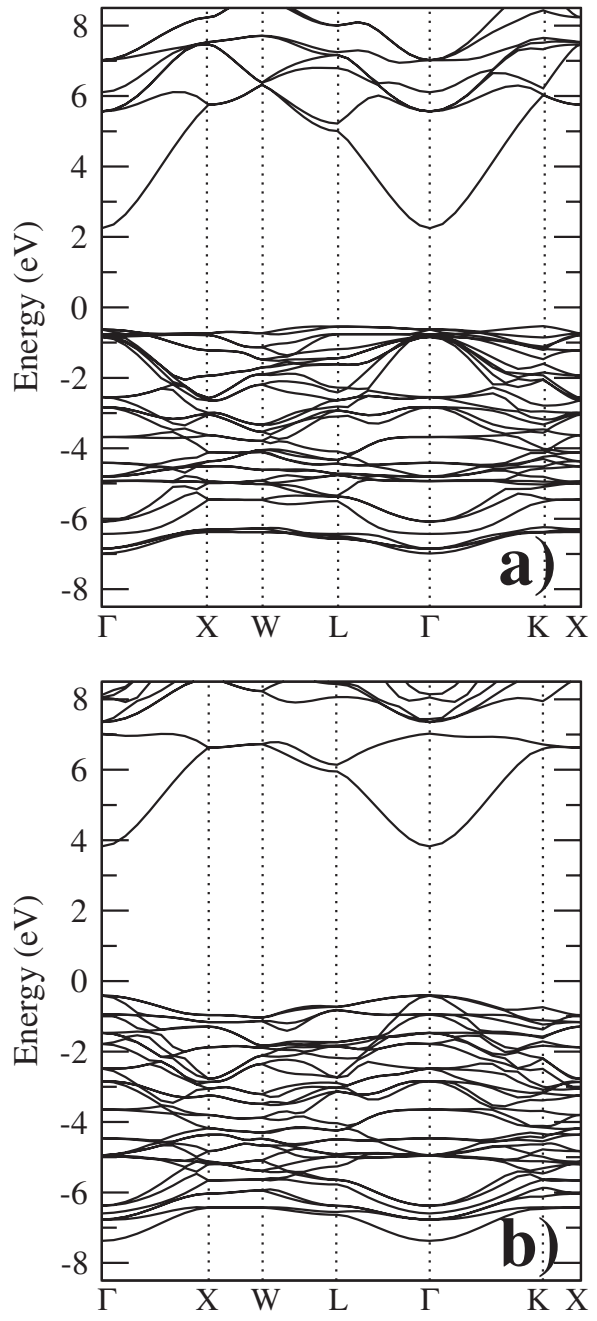

FIG. 2. Calculated band structure of (a) $ZnGa_2O_4$ and (b) $ZnAl_2O_4$ spinel structures at equilibrium volume.

band-gap semiconductors. According to Sampath and Cordaro[24] the optical-band gap derived from reflectance measurements are between 3.8–3.9 and 4.1–4.3 eV for $ZnAl_2O_4$ and $ZnGa_2O_4$, respectively.

Previous tight-binding calculations[25] obtain a direct band gap of 4.11 eV for $ZnAl_2O_4$ and 2.79 eV for $ZnGa_2O_4$. In this work, Sampath *et al.*[25] suggested that the band gap in Ref. 24 for $ZnAl_2O_4$ is probably incorrect. Other linear-augmented plane-waves studies from Pisani *et al.*[6] for $ZnGa_2O_4$ report a band gap at the Γ point of 2.7 eV, with no indication about if it is direct or indirect. In our calculations the $ZnAl_2O_4$ has a direct band gap, Γ-Γ, of 4.24 eV while $ZnGa_2O_4$ has an indirect band gap, *K*-Γ, of 2.78 eV, in good agreement with previous theoretical results.[6,11,25] In $ZnGa_2O_4$, the presence of the occupied Ga 3*d* state is the origin of the indirect gap, due to the symmetry-forbidden Ga 3*d*-O 2*p* coupling at the Γ point. Of course, it is well-known that LDA systematically underestimates the band gap, but the symmetry and the pressure evolution of the band gap are usually well described.

TABLE II. Calculated vibrational-modes (cm^{-1}) for $ZnGa_2O_4$ and $ZnAl_2O_4$ at zero pressure in the Γ point.

Species	$ZnGa_2O_4$	$ZnAl_2O_4$
T_{2u}	135	250
T_{1u}(IR)	175	222
$T_{2g}(R)$	186	194
E_u	229	402
T_{1u}(IR)	342	496
T_{1g}	366	371
$E_g(R)$	395	427
A_{2u}	419	672
T_{1u}(IR)	429	548
T_{2u}	450	484
$T_{2g}(R)$	488	513
E_u	563	600
T_{1u}(IR)	580	666
$T_{2g}(R)$	618	655
A_{2u}	702	769
$A_{1g}(R)$	717	775

Cubic spinels $ZnAl_2O_4$ and $ZnGa_2O_4$ belong to the space-group 227 and have 2 f.u. per primitive cell. The phonon modes at the Γ point are classified as follows:[26]

$$\Gamma = A_{1g}(R) + E_g(R) + T_{1g} + 3T_{2g}(R) + 2A_{2u} + 2E_u + 4T_{1u}(\mathrm{IR}) + 2T_{2u},$$

where *R* and IR corresponds to Raman and infrared-active modes, respectively. Our calculated phonon frequencies at zero pressure are listed in Table II.

The experimental Raman and IR active modes obtained by Manjon[27] and Gorkom *et al.*[28] for $ZnGa_2O_4$, Chopelas and Hofmeister,[26] and the theoretical data from Fang *et al.*[9] for $ZnAl_2O_4$ are listed in Table III. In general, there is fair agreement for $ZnAl_2O_4$ between available experimental, previous theoretical data and our results, with a slight deviation of 0.5%–2.4% in the Raman-active modes. In the case of $ZnGa_2O_4$, to our knowledge, there is no previous first-principles study of Raman frequencies, even though we can report good agreement with available experimental data, except for the E_g mode from Ref. 28. In particular, we obtain a frequency of E_g=395 cm^{-1} which happens to be in good agreement with other experimental values reported for other spinel compounds such as $ZnAl_2O_4$ and $MgAl_2O_4$.[26]

The role of the cations in the phonon frequencies of $MgAl_2O_4$, $ZnAl_2O_4$, and $ZnGa_2O_4$ can be understood from the cation masses. Mainly because the A^{2+} (Mg^{2+} and Zn^{2+}) cations have a similar ionic radius and local bonding envi-

TABLE III. Comparison between calculated and experimental Raman and IR-active modes (cm^{-1}) of $ZnGa_2O_4$ and $ZnAl_2O_4$.

Modes	$ZnGa_2O_4$	Exp.[a]	Exp.[b]	$ZnAl_2O_4$	Exp.[c]	Theory[d]
			Raman			
T_{2g}	186			194	196	197
E_g	395		638	427	417	442
T_{2g}	488	462	467	513	509	520
T_{2g}	618	606	611	655	658	665
A_{1g}	717	706	714	775	758	785
			IR			
T_{1u}	175		175	222	220(231)	226(240)
	342		328	496	440(533)	507(528)
	429		420	548	543(608)	562(648)
	580		570	666	641(787)	675(832)

[a]Reference 27.
[b]Reference 28.
[c]Reference 26.
[d]Reference 9.

ronment, the same occurs for the cation B^{3+} (Al^{3+} and Ga^{3+}). The differences on the phonon frequencies are larger by considering different cations B^{3+} than cations A^{2+}. As an example, we compare the Raman-active modes (T_{2g}, E_g, T_{2g}, T_{2g}, and A_{1g}) of $MgAl_2O_4$ (312, 407, 492, 666, and 767 cm^{-1}), $ZnAl_2O_4$ (196, 417, 509, 658, and 768 cm^{-1}),[26] and $ZnGa_2O_4$ (186, 395, 462, 606, and 706 cm^{-1} from our results and Ref. 27) (see Table III). It is clear that the absolute frequency difference, between the theoretical and the experimental data, is bigger when the B^{3+} cation is changed, mainly for the second and third T_{2g} and A_{1g} active modes.

B. High-pressure phases

In order to show the behavior of the structural parameters under pressure for $ZnAl_2O_4$ and $ZnGa_2O_4$, the equilibrium geometries of these cubic spinel compounds were studied up to a pressure of around 50 GPa, in steps of ≈2.5 GPa. Optimization of internal coordinates at each pressure was performed. The variations in the lattice-parameter a and oxygen parameter u, with respect to the pressure, are shown in Fig. 3. The behavior of a is almost the same for both compounds, while the variation in u is more important for $ZnGa_2O_4$. This difference can be explained by looking at the dependence on the structural changes with respect to the masses differences of the B^{3+} cation for both compounds. It is shown in Table I that at zero pressure the distances $d_{Zn\text{-}O}$ and $d_{X\text{-}O}(X=Al,Ga)$ have a larger difference in $ZnGa_2O_4$ than in $ZnAl_2O_4$. Figure 4 shows that $d_{Zn\text{-}O}$ decreases faster with pressure than $d_{X\text{-}O}$, and also evidences that $d_{Zn\text{-}O}$ is larger than $d_{X\text{-}O}$ in $ZnAl_2O_4$ while the converse is true for $ZnGa_2O_4$. We conclude, in general, that as the pressure increases, the absolute distance $d_{Zn\text{-}O}$ and $d_{X\text{-}O}$, in $ZnAl_2O_4$, gets closer to each other, while the opposite behavior is presented in $ZnGa_2O_4$.

According to Ono *et al.*,[29] the spinel $MgAl_2O_4$ decomposes into an assemblage of periclase (MgO) and corundum (Al_2O_3) at pressures above 15 GPa. This behavior has not been observed in experiments on $ZnAl_2O_4$ or $ZnGa_2O_4$. In order to test this possibility, we probe the configurations periclase+corundum as in Ref. 2 (for $MgAl_2O_4$) for both spinels, and we have found that this possibility is not energetically competitive.

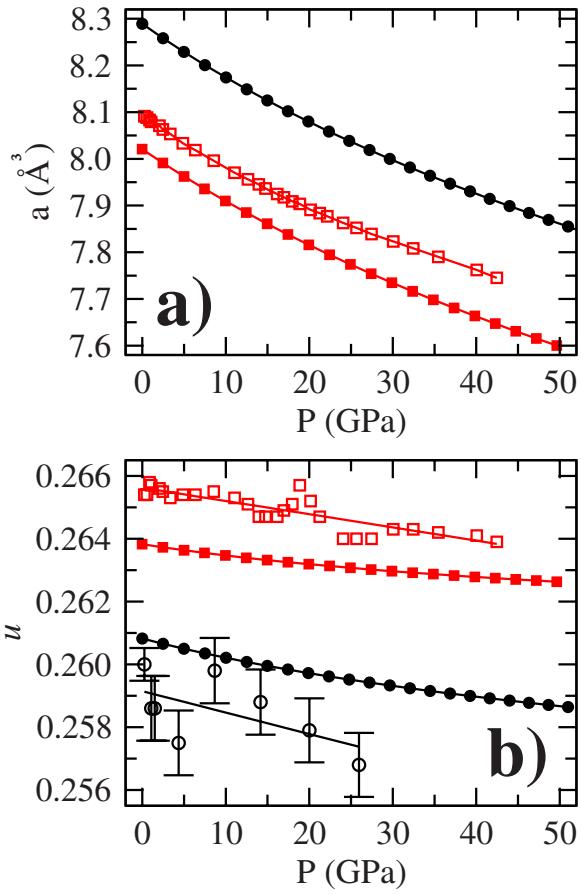

FIG. 3. (Color online) Pressure dependence of the (a) lattice-parameter a and (b) oxygen-parameter u of the spinels $ZnAl_2O_4$ and $ZnGa_2O_4$ compounds up to 50 GPa. In both figures, the labels for $ZnGa_2O_4$ are as follows: black-filled circles for theoretical and black open circles for experimental data; and for $ZnAl_2O_4$: red-filled squares for theoretical and red open squares for experimental data. The experimental data are taken from Refs. 3 and 5.

The first phase transition obtained by Errandonea *et al.*[5] in $ZnGa_2O_4$ appears at 31.2 GPa from cubic spinel to a tetragonal spinel structure without changes in volume and $c/a=1.398$, clearly different from the ideal value $c/a=\sqrt{2}$. The lattice parameters for the different phases from Ref. 5 and our theoretical results are listed in Table IV. The second first-order phase transition was obtained at 55.4 GPa,[5] where they have suggested that a better agreement between the observed and calculated patterns is achieved by considering a $CaMn_2O_4$-type structure (marokite), with an estimated volume collapse of around 7% at the transition pressure.

Following the path explained in Ref. 5 we find that the tetragonal spinel structure has almost the same energy than the cubic spinel structure with $c/a=1.4142$, almost equal to the ideal value $c/a=\sqrt{2}$. It means that under hydrostatic conditions the tetragonal structure reduces to the cubic spinel

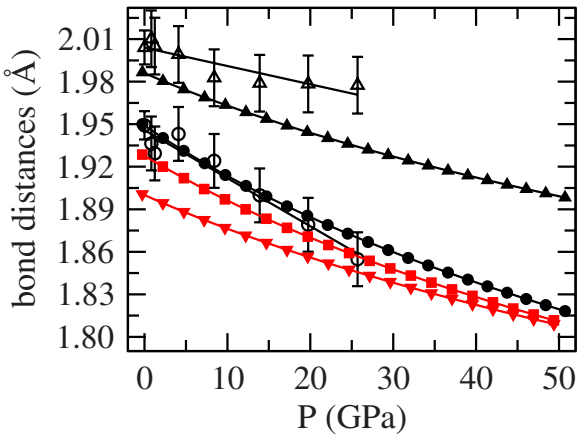

FIG. 4. (Color online) Pressure dependence of the bond-distances $d_{Zn\text{-}O}$, $d_{Ga\text{-}O}$, and $d_{Al\text{-}O}$, of the spinel structures up to 50 GPa. The labels are as follows, for $d_{Zn\text{-}O}$ in $ZnGa_2O_4$: black-filled circles for theoretical and black open circles for experimental data (Ref. 5); and black-filled triangles up for theory and black open triangles for experimental data for $d_{Ga\text{-}O}$. For theoretical values of $ZnAl_2O_4$ the labels are: red-filled squares for $d_{Zn\text{-}O}$ and red triangles down for $d_{Al\text{-}O}$.

phase. In order to test the effect of nonhydrostatic conditions, we performed similar calculations at 32 GPa by imposing the c/a values reported in experiments from Ref. 5. Our results show that at this pressure the tetragonal phase, under nonhydrostatic conditions, is competitive in energy with the hydrostatic one. It means that probably the nonhydrostatic conditions can play an important role in the experiments performed by Errandonea *et al.*[5] This result would correspond to the observed first phase-transition that corresponds to a second-order type without volume changes as reported in experiments.[5]

In the second step the marokite (SG: *Pbcm*), $CaFe_2O_4$-type (SG: *Pnma*), and $CaTi_2O_4$-type (SG: *Cmcm*) structures were used to search a possible candidate to the second phase transition from the tetragonal to orthorhombic structure suggested by experiments. The Fig. 5 shows the

TABLE IV. Lattice parameters from all the structures studied. The parameters of SGs $Fd\bar{3}m$ and I_{41}/amd are from equilibrium volume, while parameters of *Pnma*, *Pbcm*, and *Cmcm* structures are at the volumes of transition pressure.

	SG	a (Å)	b (Å)	c (Å)	c/a	u
$ZnAl_2O_4$	$Fd\bar{3}m$	8.020				0.2638
	I_{41}/amd	5.671		8.021	1.414	
	Pnma	2.661	9.548	8.236		
$ZnGa_2O_4$	$Fd\bar{3}m$	8.289				0.2608
	I_{41}/amd	5.861		8.290	1.414	
	Pbcm	2.760	9.245	9.156		
Exp. (Ref. 5)	$Fd\bar{3}m$	8.341				0.2599
	I_{41}/amd	5.743		8.032	1.398	
	Pbcm	2.93	9.13	8.93		

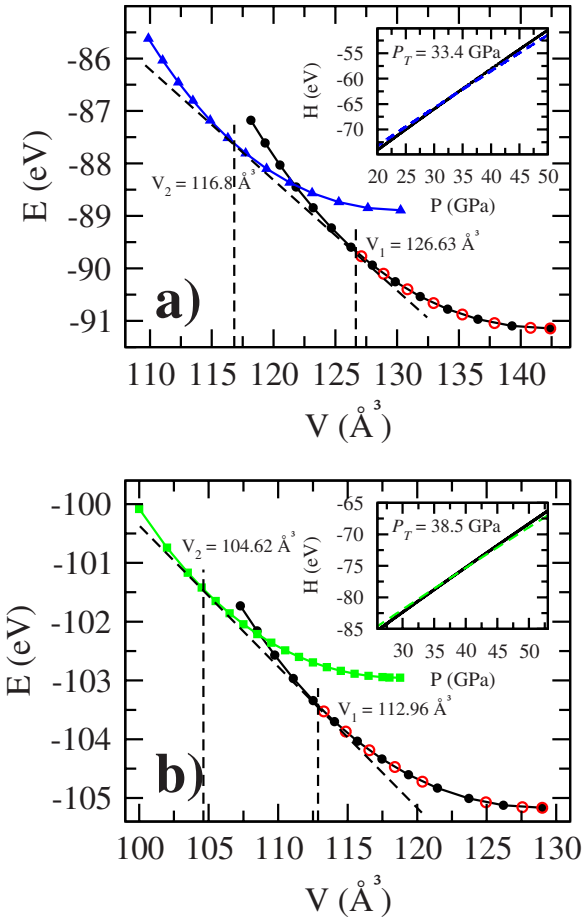

FIG. 5. (Color online) Calculated energy-volume curves of (a) $ZnGa_2O_4$ and (b) $ZnAl_2O_4$. The labels are black-filled circles for cubic spinel ($Fd\bar{3}m$), red open circles for tetragonal spinel (I_{41}/amd), green-filled squares for orthorhombic *Pnma*, and blue triangles up for orthorhombic *Pbcm*. Where V_1 and V_2 are the volumes at the transition pressure. The inset shows the enthalpy vs pressure curves in which the black solid lines are for spinel structure, blue dashed line in (a) for *Pbcm* and green dashed line in (b) for *Pnma*; The volume and energy are given per two unit formula.

calculated energy-volume curves of $ZnAl_2O_4$ and $ZnGa_2O_4$ compounds for the $Fd\bar{3}m$-, I_{41}/amd-, *Pnma*-, and *Pbcm*-analyzed structures. The insets show the variation in enthalpy with pressure of spinel in black solid line, blue dashed line for marokite in (a), and green dashed line for *Pnma* in (b). Also, this figure shows the theoretical transition pressure, P_T, at the structural phase transition.

Our results for $ZnGa_2O_4$ show that the $CaFe_2O_4$-type structure is not competitive for any pressure, while the marokite and the $CaTi_2O_4$-type structures have almost the same energy, and from the energetic point of view both are good candidates to explain the second transition.

We conclude, by comparing with experimental results, the marokite structure gives the best agreement with the observed diffraction data. Besides, the structural parameters that we obtain for the marokite structure are in good agreement with experimental measurements, as seen in Table IV. Lattice parameters of marokite structure from Table IV corresponds to the volume at the phase transition. Figure 6 sum-

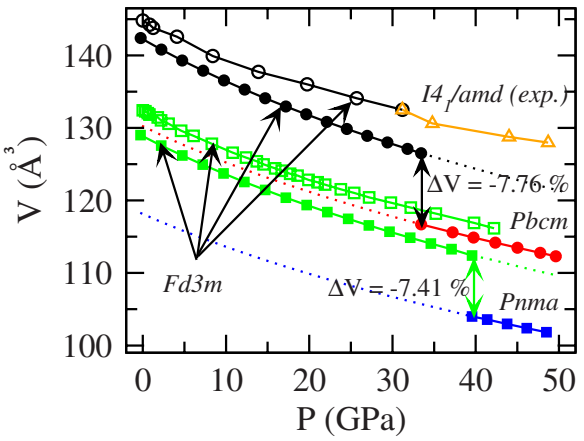

FIG. 6. (Color online) Path of the phase transition from cubic spinel to orthorhombic structures, for $ZnAl_2O_4$: green-blue-filled squares for theory, and green open squares for experimental data (Ref. 3); $ZnGa_2O_4$: black-red-filled circles for theory, and black open circles ($Fd\bar{3}m$), orange-filled triangle up (I_{41}/amd) for experimental data (Ref. 5). The volume collapse at the transition pressure are 7.41% and 7.76% in $ZnAl_2O_4$ and $ZnGa_2O_4$, respectively.

marizes our findings and shows the path of the phase transition in a pressure-volume plot from spinel to orthorhombic marokite-type structure in $ZnGa_2O_4$. According to Fig. 6, $ZnGa_2O_4$ has a volume collapse of 7.76%, in good agreement with results from Ref. 5. Our theoretical transition pressure is lower than the experimental one, but as it is known, the equal enthalpy construction usually gives lower pressure transitions that the experimental ones.[30] Also, the big difference between the experimental and theoretical transition pressure can be explained from the possible existence of kinetic barriers that are not included in the calculations. Also, the experimental nonhydrostatic conditions can play a role in the value of the observed transition pressure. It is well-known that the transition pressures reported by x-ray diffraction experiments are higher than transition pressures reported by Raman experiments under pressure.[30] We believe that future Raman experiments will obtain a lower transition pressure in better agreement with our calculations.

The cubic spinel-$ZnAl_2O_4$ structure was characterized experimentally by Levy *et al.*[3] up to a pressure of 43 GPa with no observation of a phase transition. We have performed a similar study for the $ZnAl_2O_4$ spinel. Our results demonstrate a similar behavior as with $ZnGa_2O_4$, in particular with respect to the potential phase transition between the cubic to the tetragonal spinel. For such purpose, we have performed calculations under nonhydrostatic conditions at 36 GPa by imposing a c/a value similar to the case of $ZnGa_2O_4$, and we found that the tetragonal spinel structure is competitive in energy with the hydrostatic one, as reported in Table IV and Fig. 5. It may suggest that probably under nonhydrostatic conditions this second-order phase transition could be observed. We also have performed total-energy calculations for different candidate structures for a possible first-order phase transition. In particular, we tried with structures *Pbcm*, *Pnma*, and *Cmcm*. Our results show that in this case, a first-order phase transition occurs at 38.5 GPa in $ZnAl_2O_4$ from cubic spinel to a *Pnma* structure, while the marokite-type structure is not competitive. Again, like in $ZnGa_2O_4$, probably due to the kinetic barriers, the experimental transition pressure would be higher and this transition was not observed by Levy *et al.*;[3] we expect that high-pressure experiments over 50 GPa will observe these transitions.

The cubic-spinel $ZnAl_2O_4$, under pressure, has a first phase transition to the $CaFe_2O_4$-type structure. This high-pressure phase also appears in $MgAl_2O_4$. From the experimental study[5] and our results, $ZnGa_2O_4$ under pressure goes to the marokite structure. This different behavior can be understood due to the replacement of the cation B (Al or Ga), in fact it is well-known the role of the d electron in many semiconductor compounds under pressure.[30,31]

In regards to the cation coordination, we observe an increase from 4 to 8 in Zn coordination in $ZnAl_2O_4$ and $ZnGa_2O_4$, at high-pressure phases. Both orthorhombic structures are made up of BO_6 (B=Al or Ga)- distorted octahedra and ZnO_8 zinc-centered distorted polyhedra (see Fig. 1).

IV. CONCLUSIONS

In summary, we have performed first-principles calculations to study structural, electronic, and vibrational properties for cubic spinels $ZnAl_2O_4$ and $ZnGa_2O_4$ at zero pressure. The results are in good agreement with previous reported calculations and with the available experimental data. With respect to vibrational characterization, we report the zone-center phonon frequencies at zero pressure of both cubic spinels.

We found that $ZnGa_2O_4$ and $ZnAl_2O_4$ spinel compounds can have a second-order phase transition from cubic to tetragonal spinel I_{41}/amd under nonhydrostatic conditions. When increasing pressure the $ZnGa_2O_4$ has a first-order phase transition to a marokite *Pbcm* structure at 33.44 GPa. In the case of $ZnAl_2O_4$ we predict a first-order phase transition to a *Pnma* structure at 38.5 GPa. In both cases the high-pressure phases are orthorhombic and contain BO_6 (B=Al or Ga)-distorted octahedra and ZnO_8 zinc-centered distorted polyhedra. We hope that this work will stimulate future high-pressure Raman and x-ray experiments in these compounds.

ACKNOWLEDGMENTS

A.H.R. has been supported by CONACYT Mexico under Projects J-59853-F and J-83247-F. P.R.-H and A.M. acknowledge the financial support of the MICINN of Spain under Grants No. MAT2007-65990-C03-03 and No. CSD2007-00045, and the computer resources provided by MareNostrum, Spain and Kan Balam Supercomputer, UNAM, México.

*lsinhue@qro.cinvestav.mx
†aromero@qro.cinvestav.mx
‡placida@marengo.dfis.ull.es
§amunoz@marengo.dfis.ull.es

[1] A. Reid and A. Ringwood, Earth Planet. Sci. Lett. **6**, 205 (1969).
[2] S. Ono, J. Brodholt, and G. Price, Phys. Chem. Miner. **35**, 381 (2008).
[3] D. Levy, A. Pavese, A. Sani, and V. Pischedda, Phys. Chem. Miner. **28**, 612 (2001).
[4] D. Levy, A. Pavese, and M. Hanfland, Phys. Chem. Miner. **27**, 638 (2000).
[5] D. Errandonea, R. S. Kumar, F. J. Manjon, V. V. Ursaki, and E. V. Rusu, Phys. Rev. B **79**, 024103 (2009).
[6] L. Pisani, T. Maitra, and R. Valentí, Phys. Rev. B **73**, 205204 (2006).
[7] A. Bouhemadou and R. Khenata, Phys. Lett. A **360**, 339 (2006).
[8] J. M. Recio, R. Franco, A. Martin Pendas, M. A. Blanco, L. Pueyo, and R. Pandey Phys. Rev. B **63**, 184101 (2001).
[9] C. M. Fang, C. K. Loong, G. A. de Wijs, and G. de With, Phys. Rev. B **66**, 144301 (2002).
[10] S. H. Wei and S. B. Zhang, Phys. Rev. B **63**, 045112 (2001).
[11] R. Khenata, M. Sahnoun, H. Baltache, M. Rérat, A. H. Reshak, Y. Al-Douri, and B. Bouhafs, Phys. Lett. A **344**, 271 (2005).
[12] P. E. Blochl, Phys. Rev. B **50**, 17953 (1994).
[13] G. Kresse and D. Joubert, Phys. Rev. B **59**, 1758 (1999).
[14] G. Kresse and J. Hafner, Phys. Rev. B **47**, 558 (1993).
[15] G. Kresse and J. Hafner, Phys. Rev. B **49**, 14251 (1994).
[16] G. Kresse and J. Furthmüller, Comput. Mater. Sci. **6**, 15 (1996).
[17] G. Kresse and J. Furthmüller, Phys. Rev. B **54**, 11169 (1996).
[18] J. P. Perdew and A. Zunger, Phys. Rev. B **23**, 5048 (1981).
[19] H. Monkhorst and J. Pack, Phys. Rev. B **13**, 5188 (1976).
[20] K. Parlinski, Computer Code PHONON http://wolf.ifj.edu.pl/phonon).
[21] F. Murnaghan, Proc. Natl. Acad. Sci. U.S.A. **30**, 244 (1944).
[22] J. P. Perdew, K. Burke, and M. Ernzerhof, Phys. Rev. Lett. **77**, 3865 (1996).
[23] J. Perdew, K. Burke, and M. Ernzerhof, Phys. Rev. Lett. **78**, 1396 (1997).
[24] S. K. Sampath and J. F. Cordaro, J. Am. Ceram. Soc. **81**, 649 (1998).
[25] S. Sampath, D. Kanhere, and R. Pandey, J. Phys.: Condens. Matter **11**, 3635 (1999).
[26] A. Chopelas and A. Hofmeister, Phys. Chem. Miner. **18**, 279 (1991).
[27] F. J. Manjon, private communication.
[28] G. G. P. van Gorkom, J. H. Haanstra, and H. van den Boom, J. Raman Spectrosc. **1**, 513 (1973).
[29] S. Ono, T. Kikewaga, and Y. Ohishi, Phys. Chem. Miner. **33**, 200 (2006).
[30] A. Mujica, A. Rubio, A. Munoz, and R. Needs, Rev. Mod. Phys. **75**, 863 (2003).
[31] S. H. Wei and A. Zunger, Phys. Rev. B **60**, 5404 (1999).